# Reactions of N($^2$D) with Polycyclic Aromatic Hydrocarbons: A Computational Approach

Marzio Rosi[1,2(✉)], Nadia Balucani[3], Luca Mancini[3], Giacomo Pannacci[3], Marco Parriani[3], Dimitrios Skouteris[4], and Gianmarco Vanuzzo[3]

[1] Dipartimento di Ingegneria Civile ed Ambientale, Università di Perugia, 06125 Perugia, Italy
marzio.rosi@unipg.it
[2] Istituto CNR di Scienze e Tecnologie Chimiche "Giulio Natta" (CNR-SCITEC), 06123 Perugia, Italy
[3] Dipartimento di Chimica, Biologia e Biotecnologie, Università di Perugia, 06123 Perugia, Italy
{nadia.balucani,luca.mancini,giacomo.pannacci,marco.parriani, gianmarco.vanuzzo}@unipg.it
[4] Master-Tec srl, 06128 Perugia, Italy

**Abstract.** Investigating large polycyclic aromatic hydrocarbons (PAHs) in interaction with atomic nitrogen poses a major computational challenge due to the high demands on processing time and temporary storage space. Highly precise approaches, such as CCSD(T) paired with extensive basis sets, are often impractical. This paper explores a cost-effective computational approach that delivers sufficiently reliable outcomes without excessive resource needs.

Specifically, we employ the ONIOM method developed by Morokuma and colleagues. This involves a two-layer ONIOM scheme, where the high-level layer applies the CCSD(T) method with the aug-cc-pVTZ basis set, while the low-level layer uses the hybrid B3LYP functional paired with the aug-cc-pVTZ basis set. The strategy is implemented to model the interaction between N($^2$D) and both naphthalene and phenanthrene.

**Keywords:** Computational chemistry · ONIOM · Density Functional Theory methods · Coupled Cluster calculations · Potential energy surface

## 1 Introduction

Atomic nitrogen in its ground state ($^4$S) exhibits very low reactivity toward closed-shell molecules such as hydrocarbons, whereas in its first electronically excited $^2$D state, it displays substantial reactivity with hydrocarbons. N($^2$D) was detected in the water-poor comet C/2016 R2 (Pan-STARRS) [1] and in a plethora of strongly photon-irradiated environments including the Orion Nebula (M42), low-ionization H II regions (M43), planetary nebulae (*i.e.* the Ring Nebula), supernova remnants (*i.e.* the Crab Nebula), and Herbig-Haro objects [2–5]. Polycyclic aromatic hydrocarbons and similar compounds are thought to be ubiquitous throughout the interstellar medium (ISM), with aromatic chemistry playing a prominent role from the initial phases of star formation.

© The Author(s), under exclusive license to Springer Nature Switzerland AG 2027
O. Gervasi et al. (Eds.): ICCSA 2026 Workshops, LNCS 16760, pp. 440–452, 2027.
https://doi.org/10.1007/978-3-032-30521-3_28

Nitrogen, in its molecular form, and hydrocarbons, both aliphatic and aromatic, are also the main components of the atmosphere of Titan [6, 7]. This atmosphere is similar, in some aspects, to the primordial atmosphere of Earth [8, 9] and for this reason has been extensively studied by several missions [10, 11]. Among the hydrocarbons identified on Titan there is benzene [12, 14]. Dinitrogen in the atmosphere of Titan can dissociate into atomic nitrogen both in its ground state or $^2$D excited state in similar amounts [15, 16] and N ($^2$D) can easily react with other constituents of the upper atmosphere of Titan or with species present in the ISM [17–24].

The reaction of N($^2$D) with several aliphatic hydrocarbons of increasing complexity, starting from methane, has been already investigated both theoretically, using accurate ab initio methods and kinetic calculations, and experimentally, through crossed molecular beams techniques [25–32]. A similar approach is employed for the reactions between N($^2$D) and aromatic hydrocarbons, starting from benzene [33–35] and toluene [36, 37] with the intention to extend the study to more complex aromatic systems, like polycyclic aromatic hydrocarbons (PAHs).

In this contribution we will present a computational strategy to study large systems as those relative to the interaction of nitrogen in its excited $^2$D state and polycyclic aromatic hydrocarbons, in particular naphthalene and phenanthrene. We will use the previously investigated system N($^2$D) + $C_6H_6$ as a benchmark calculation in order to establish the better approach for the investigation of larger systems [35, 38].

## 2 Computational Details

The optimization of the stationary points of the Potential Energy Surface (PES) of N($^2$D) interacting with benzene, naphthalene and phenanthrene has been performed at Density Functional Theory (DFT) level of calculation using the B3LYP [39, 40] functional and the 6–311 + G(d,p) basis set [41, 42], with the addition of the D3 dispersion [43]. For benzene the DFT geometry optimizations were performed also using the aug-cc-pVTZ basis set [44]. In order to assign the saddle points to the relative reactants and products, we performed intrinsic reaction coordinate (IRC) calculations [45, 46]. The energy of all the stationary points of N($^2$D) + benzene and naphthalene was computed also at the CCSD(T) level [47–49] using the correlation consistent aug-cc-pVTZ basis set [44]. The energy of N($^2$D) has been estimated by adding the experimental [50] separation N($^4$S) – N($^2$D) of 230 kJ mol$^{-1}$ to the energy of N($^4$S) at all levels of calculations. The zero point energy correction (ZPE) computed using the DFT vibrational frequencies has been added at all level of calculation. A similar computational scheme has been previously successfully applied [51–56].

More precise computations were carried out for the stationary points of the N($^2$D) + benzene system at the CCSD(T) level. These included corrections from density-fitted (DF) MP2 extrapolation to the complete basis set, along with corrections for core electron excitations. In particular, we compute the energies as:

$$E_{CCSD(T)/CBS} = E(CCSD(T)/aug-cc-pVTZ) + \left[E(CCSD(T,core)/cc-pVTZ) - E(CCSD(T)/cc-pVTZ)\right] + \left[E(DF-MP2/CBS) - E(DF-MP2/aug-cc-pVTZ)\right]$$

where E(DF-MP2/CBS) is defined as:

$$\mathrm{E(DF-MP2/CBS)} = \mathrm{E}\big[\,(\mathrm{DF-MP2})/\mathrm{aug-cc-pVQZ})\big] + 0.5772* \\ [\mathrm{E(DF-MP2/aug-cc-pVQZ)} - \mathrm{E(DF-MP2/aug-cc-pVTZ)}]$$

The E(DF-MP2/CBS) extrapolation was performed using Martin's two parameter scheme [57]. These energies will be denoted as CCSD(T)/CBS although they include also the core-valence correlation correction. The accuracy of these calculations should be within ± 5 kJ/mol. This approach is computationally unfeasible for the systems $N(^2D)$ + naphthalene or phenanthrene. For this last system also CCSD(T)/aug-cc-pVTZ calculations are unfeasible, being too expensive as far as computational resources are concerned.

For these reasons, we decided to explore the opportunities provided by the ONIOM approach for the investigation of $N(^2D)$ + naphthalene and phenanthrene. We used the ONIOM method of Morokuma and co-workers [58–60]. We used a two level ONIOM approach, with the hybrid B3LYP approach in conjunction with the aug-cc-pVTZ basis set being used for the low level treatment and the CCSD(T)/aug-cc-pVTZ for the high level treatment. The high level treatment is applied to nitrogen and the ring involved in the interaction, while the rest of the PAH is described at the low level treatment. The dangling bonds are replaced by hydrogens. The computational cost of this treatment is comparable to that of the system $N(^2D) + C_6H_6$.

The DFT and CCSD(T) calculations were done with Gaussian 09 [61] and the CCSD(T)/CBS calculations with Molpro [62, 63], while the analysis of the vibrational frequencies was performed using Molekel [64, 65].

## 3 Results and Discussion

### 3.1 $N(^2D)$ + Benzene

In Fig. 1 we have reported the Potential Energy Surface (PES) relative to the lowest exit channel of the reaction of $N(^2D)$ and benzene. The complete PES has been previously published [35]. The approach of $N(^2D)$ to the benzene ring gives rise to a first intermediate (B-w1) which evolves through a low transition state to a more stable species (B-w2) with the nitrogen bonded to two carbon atoms. This species evolves with the insertion of nitrogen into the C—C bond giving rise to a 7-membered ring (B-w3). The 7-membered ring evolves through minima B-w4 and B-w5 giving rise to the final products, HCN and cyclopentadienyl radical. In Fig. 1 we have reported the energies relative to $N(^2D) + C_6H_6$ computed at different level of accuracy: B3LYP with an aug-cc-pVTZ basis set [44], coupled cluster with inclusion of triple excitations (CCSD(T)) with the same aug-cc-pVTZ basis set and CCSD(T) with an extrapolation to complete basis set limit (CBS) and inclusion also of the core-valence correlation effects. This last approach is extremely accurate and provides results with an error which can be estimated lower than $\pm 5$ kJ mol$^{-1}$. However, this accuracy has a very high computational cost in terms of CPU time and disk space. For this reason this approach can be applied only to relatively small systems and cannot be applied, for instance, to the study of the interaction of $N(^2D)$ with polycyclic aromatic hydrocarbons. We can use, however, these results as benchmark calculations in order to choose the best approach to the study of larger systems.

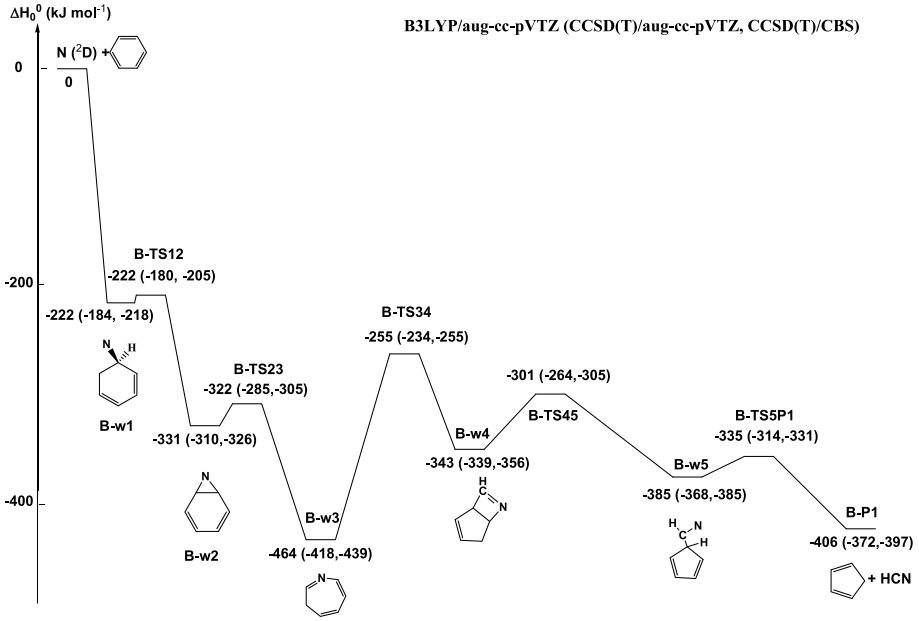


**Fig. 1.** PES for the N($^2$D) + benzene reaction. Relative energies (kJ mol$^{-1}$) with respect to N($^2$D) + benzene, computed at B3LYP/aug-cc-pVTZ, CCSD(T)/aug-cc-pVTZ and CCSD(T)/CBS level. Zero point energy correction always included.

From the values reported in Fig. 1 we can notice that CCSD(T)/aug-cc-pVTZ relative energies are higher than B3LYP energies by an average of 28 kJ mol$^{-1}$, while CCSD(T)/CBS energies are lower than CCSD(T) energies by an average of 23 kJ mol$^{-1}$. Indeed, most of the times there is a better agreement between B3LYP and CCSD(T)/CBS results with respect to CCSD(T)/aug-cc-pVTZ and CCSD(T)/CBS results. Unfortunately, the discrepancy between B3LYP and more accurate results is not always the same. For this reason it is necessary to perform more accurate calculations as CCSD(T), but we must be aware that CCSD(T) calculations converge on basis set very slowly and CCSD(T) calculations even with an extended basis set as the aug-cc-pVTZ show a basis set incompleteness error. In this case this error is around 20 kJ mol$^{-1}$.

### 3.2 N($^2$D) + Naphthalene

In Fig. 2 we have reported the geometries of the stationary points of the lowest exit channel of the PES relative to the reaction of N($^2$D) with naphthalene, optimized at B3LYP/6–311 + G(d,p) level. The PES relative to the lowest exit channel has been reported in Fig. 3, while the complete PES has been published elsewhere [66].

The interaction of N($^2$D) with naphthalene gives rise to species N-w3 where the nitrogen atom is already inserted into the C—C bond with the formation of a 7-membered ring. This species evolves through minima N-w4 and N-w5 to the exit channel where we have the formation of HCN. This reaction, except for the initial approach of nitrogen to the naphthalene, is very similar to the reaction of nitrogen and benzene. The second ring of

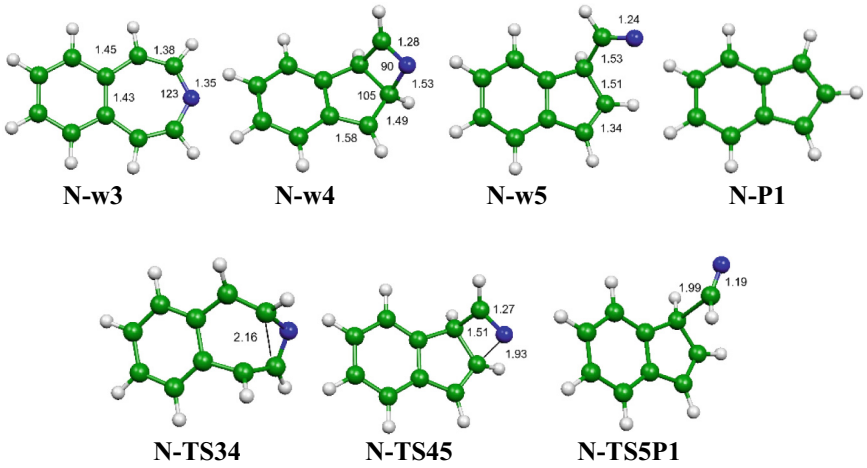


**Fig. 2.** Optimized geometries of the stationary points for the N($^2$D) + naphthalene PES, computed at B3LYP/6-311 + G(d,p) level. Bond lengths in Å, angles in °.

naphthalene indeed acts as a spectator. This is confirmed by the optimized geometries of naphthalene and N-w3 reported in Fig. 4. From Fig. 4 we can notice that the geometrical parameters of the second ring (that is the ring not interacting with nitrogen) are almost the same in naphthalene and in the N-w3 minimum where the 7-membered ring is already formed. This consideration suggests a new computational approach for this system. We decided therefore to use a two level computational method as ONIOM, describing at an higher level as CCSD(T)/aug-cc-pVTZ the reactive part of the system (in this case the ring interacting with nitrogen and the nitrogen itself) and at a lower level as B3LYP/aug-cc-pVTZ the spectator ring. The computational cost in this case is comparable to that afforded for the system N($^2$D) + benzene. In Fig. 3 we have reported the ONIOM energies in parentheses. For comparison we have performed also CCSD(T)/aug-cc-pVTZ calculations for the whole system and we have obtained energy values very close to those obtained at the ONIOM level. This confirms that the results of the ONIOM calculations are comparable to the results obtained applying the higher level method to the whole system. The results obtained with ONIOM of course present an error due to basis set incompleteness, but we can estimate this error using the N($^2$D) + benzene benchmark calculations.

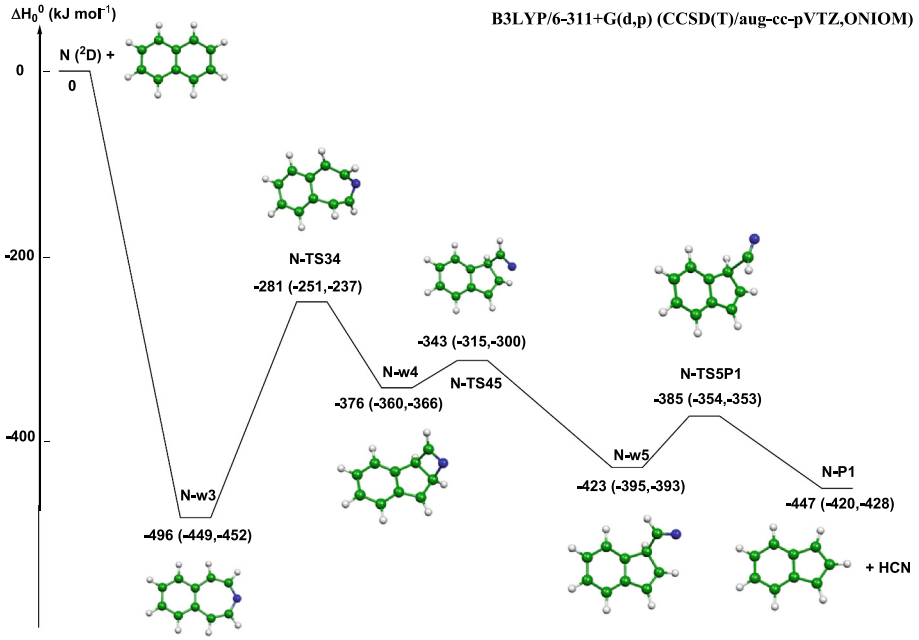


**Fig. 3.** PES for the N($^2$D) + naphthalene reaction. Relative energies (kJ mol$^{-1}$) with respect to N($^2$D) + naphthalene, computed at B3LYP/6–311 + G(d,p), CCSD(T)/aug-cc-pVTZ and ONIOM level. Zero point energy correction computed at DFT level always included.

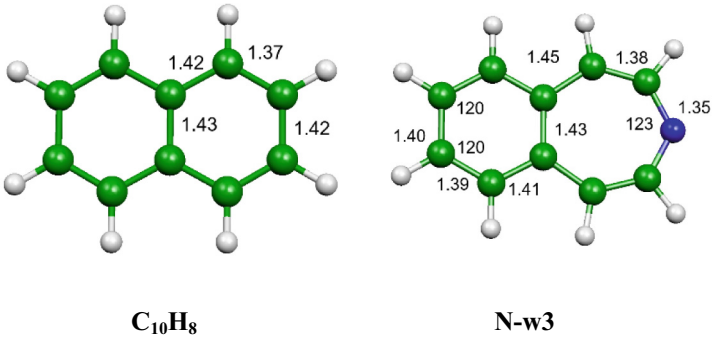


**$C_{10}H_8$** **N-w3**

**Fig. 4.** Comparison between the optimized geometries of naphthalene and N-w3, that is the minimum formed from the interaction of N($^2$D) with naphthalene. Bond lengths in Å, angles in °.

### 3.3 N($^2$D) + Phenanthrene

In Fig. 5 we have reported the geometries of the stationary points of the lowest exit channel of the PES relative to the reaction N($^2$D) and phenanthrene, optimized at B3LYP/6–311 + G(d,p) level. The PES relative to the lowest exit channel has been reported in Fig. 6, while the complete PES has been published elsewhere [66].

The interaction of N($^2$D) with phenanthrene gives rise to species P-w2 where the nitrogen atom interacts with two carbon atoms. This species evolves to minimum P-w3 where the nitrogen atom is inserted into the C—C bond with the formation of a 7-membered ring. This species evolves through minima P-w4 and P-w5 to the exit channel where we have the formation of HCN. This reaction, except for the initial approach of nitrogen to phenanthrene, is very similar to the reaction of nitrogen and benzene. The lateral rings of phenanthrene indeed act as spectators. This is confirmed by the optimized geometries of phenanthrene and P-w2 reported in Fig. 7. From Fig. 7 we can notice that the geometrical parameters of the second and third rings (that is the rings not interacting with nitrogen) are almost the same in phenanthrene and in the P-w2 minimum. We decided therefore to use also in this case a two level computational method as ONIOM, describing at an higher level as CCSD(T)/aug-cc-pVTZ the reactive part of the system (in this case the ring interacting with nitrogen and the nitrogen itself) and at a lower level as B3LYP/aug-cc-pVTZ the spectator rings. The computational cost in this case is comparable to that afforded for the system N($^2$D) + benzene. In Fig. 6 we have reported the ONIOM energies in parentheses. The results obtained with ONIOM of course present an error due to basis set incompleteness, but we can estimate this error using the N($^2$D) + benzene benchmark calculations.

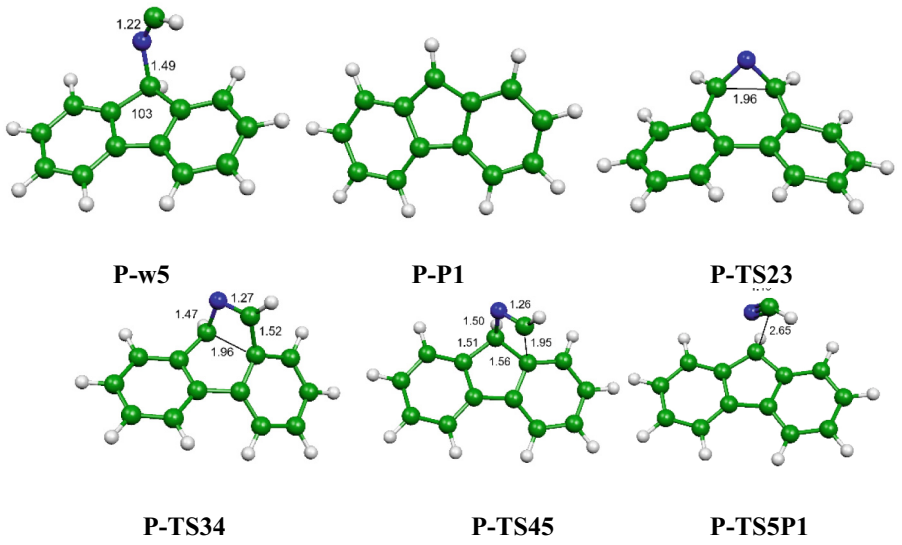


**Fig. 5.** Optimized geometries of the stationary points for the N($^2$D) + phenanthrene PES, computed at B3LYP/6-311 + G(d,p) level. Bond lengths in Å, angles in °.

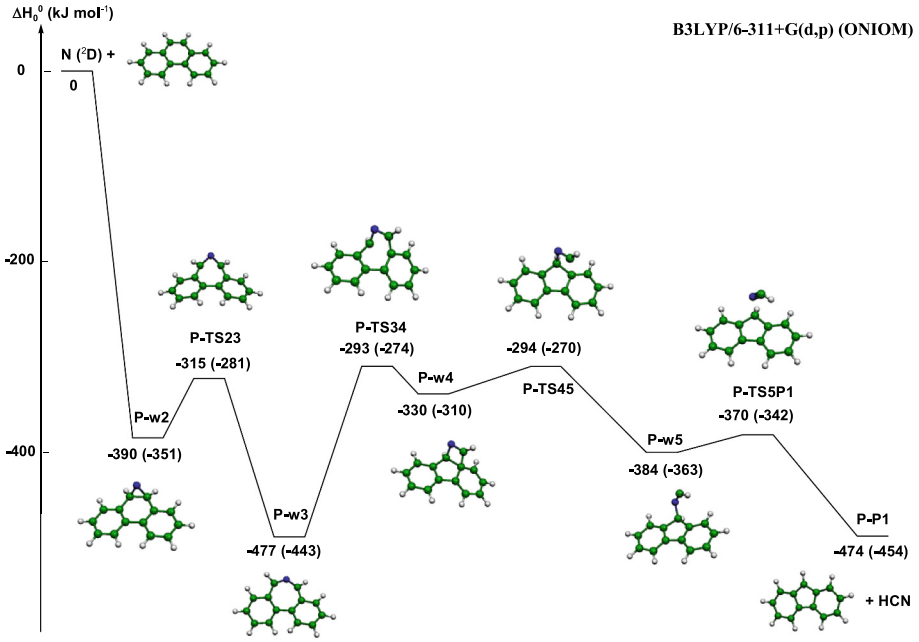


**Fig. 6.** PES for the N($^2$D) + phenanthrene reaction. Relative energies (kJ mol$^{-1}$) with respect to N($^2$D) + phenanthrene, computed at B3LYP/6-311 + G(d,p) and ONIOM level. Zero point energy correction computed at DFT level always included.

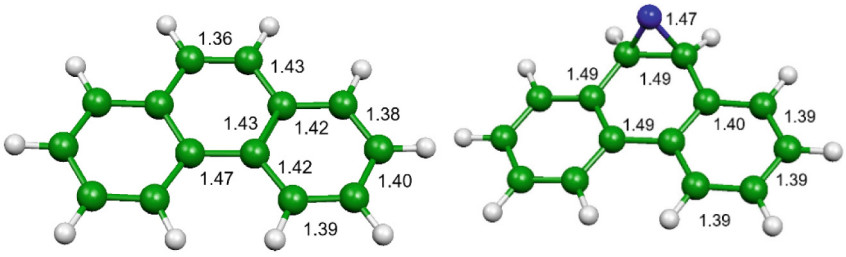


**$C_{14}H_{10}$** **P-w2**

**Fig. 7.** Comparison between the optimized geometries of phenanthrene and P-w2, that is the minimum formed from the interaction of N($^2$D) with phenanthrene. Bond lengths in Å.

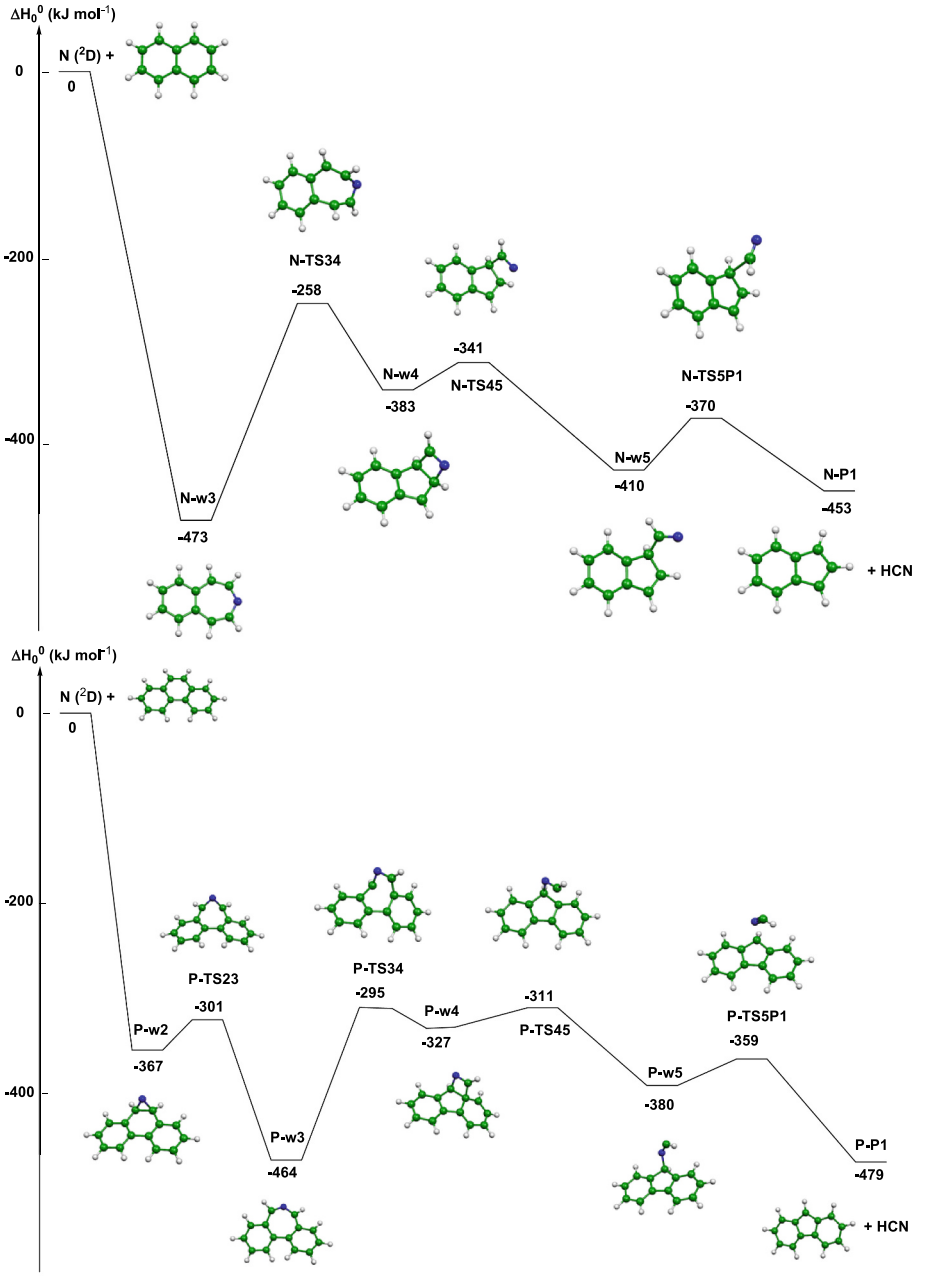


**Fig. 8.** Best estimate for the PES of N($^2$D) + naphthalene (top) and phenanthrene (bottom). Relative energies (kJ mol$^{-1}$) with respect to N($^2$D) + naphthalene or phenanthrene. Zero point energy correction computed at DFT level always included.

## 4 Conclusions

In Fig. 8 we have reported our best estimate for the lowest exit pathway for the reactions of N($^2$D) with naphthalene (top) and phenanthrene (bottom). These values were obtained adding the difference between CCSD(T)/aug-cc-pVTZ and CCSD(T)/CBS energies computed for the system N($^2$D) + benzene to the ONIOM energies computed for N($^2$D) + naphthalene and N($^2$D) + phenanthrene. Of course, we considered always stationary points (minima and transition states) of similar connectivity.

To sum up, the theoretical investigation—conducted at varying levels of complexity—of the interaction of N($^2$D) with benzene, naphthalene, and phenanthrene points to a computational approach for studying large aromatic hydrocarbons interacting with nitrogen in its first electronic excited state $^2$D. The use of the ONIOM approach with the description at an accurate level only of the reactive part of the system allows to extend the investigation also to complex PAHs. The use of benchmark calculations moreover allows to correct the final results in order to include also a correction for basis set incompleteness.

**Acknowledgments.** Support from the Italian Space Agency (Bando ASI Prot. N. DC-DSR-UVS-2022-231, Grant n.2023-10-U.0 MIGLIORA) is acknowledged. We acknowledge financial support under the National Recovery and Resilience Plan (NRRP), Mission 4, Component 2, Investment 1.1, Call for tender No. 1409 published on 14.9.2022 by the Italian Ministry of University and Research (MUR), funded by the European Union – NextGenerationEU– Project Title P20223H8CK Degradation of space technology polymers by thermospheric oxygen atoms and ions: an exploration of the reaction mechanisms at an atomistic level (ThermOPoly) – CUP J53D23014440001_- Grant Assignment Decree No. 1386 adopted on 01.09.2023 by the Italian Ministry of Ministry of University and Research (MUR). MR acknowledges financial support under the National Recovery and Resilience Plan (NRRP), Mission 4, Component 2, Investment 1.1, Call for tender No. 104 published on 2.2.2022 by the Italian Ministry of University and Research (MUR), funded by the European Union – NextGenerationEU– Project Title 2022JC2Y93 ChemicalOrigins: linking the fossil composition of the Solar System with the chemistry of protoplanetary disks – CUP J53D23001600006 - Grant Assignment Decree No. 962 adopted on 30.06.2023 by the Italian Ministry of Ministry of University and Research (MUR).

**Disclosure of Interests.** The authors have no competing interests to declare that are relevant to the content of this article.

## References

1. Raghuram, S., Hutsemekers, D., Opiton, C., Jehin, E., Bhadwaj, A., Manfroid, J.: Forbidden atomic carbon, nitrogen, and oxygen emission lines in the water-poor comet C/2016 R2 (Pan-STARRS). A&A **635**, A108 (2020)
2. Ferland, G.J., Henney, W.J., O'Dell, C.R., Porter, R.L., Van Hoof, P.A.M., Williams, R.J.R.: Pumping up the [N I] nebular lines. Astrophys. J. **757**, 79 (2012)
3. Dopita, M.A., Mason, D.J., Robb, W.D.: Atomic nitrogen as a probe of physical conditions in the interstellar medium. Astrophys. J. **207**, 102–109 (1976)
4. Ferland, G.J., Rees, M.J.: Radiative equilibrium of high-density clouds, with application to active galactic nucleus continua. Astrophys. J. **332**, 141 (1988)

5. Bautista, M.A.: Continuum fluorescence excitation of [N I] and [O I] lines in gaseous nebulae. Astrophys. J. **527**, 474–478 (1999)
6. Hörst, S. M.: Titan's atmosphere and climate. J. Geophys. Res. Planets **122**, 432482 (2017)
7. Vuitton, V., Yelle, R.V., Anicich, V.G.: The nitrogen chemistry of titan's upper atmosphere revealed. Astrophys. J. **647**, L175–L178 (2006)
8. Vuitton, V., et al.: Chemistry of Titan's atmosphere. In: Mueller-Wodarg, I., Griffith, C., Lellouch, E., Cravens, T. (eds.) Titan: Surface. Cambridge University Press, Atmosphere and Magnetosphere (2013)
9. Balucani, N.: Elementary reactions of N atoms with hydrocarbons: first steps towards the formation of prebiotic N-containing molecules in planetary atmospheres. Chem. Soc. Rev. **41**, 5473–5483 (2012)
10. Brown, R., Lebreton, J.P., Waite, J. (eds.): Titan from Cassini-Huygens. Springer, Netherlands (2010)
11. Lai, J.C.-Y., et al.: Mapping vinyl cyanide and other nitriles in Titan's atmosphere using ALMA. Astron. J. **154**(206), 1–10 (2017)
12. Vuitton, V., Yelle, R.V., Cui, J.: Formation and distribution of benzene on Titan. J. Geophys. Res. **113**, E05007 (2008)
13. Clark, R.N., et al.: Detection and mapping of hydrocarbon deposits on Titan. J. Geophys. Res. **115**, E10005 (2010)
14. Loison, J.C., Dobrijevic, M., Hickson, K.M.: The photochemical production of aromatics in the atmosphere of Titan. Icarus **329**, 55–71 (2019)
15. Lavvas, P., et al.: Energy deposition and primary chemical products in Titan's upper atmosphere. Icarus **213**, 233–251 (2011)
16. Dutuit, O., et al.: Critical review of N, $N^+$, $N_2^+$, $N^{++}$ and $N_2^{++}$ main production processes and reactions of relevance to Titan's atmosphere. Astrophys. J. Suppl. Ser. **204**, 20 (2013)
17. Balucani, N.: Nitrogen fixation by photochemistry in the atmosphere of titan and implications for prebiotic chemistry. In: Rodriguez, J.M., Raulin, F., Muller, C., Nixon, C. (eds.) The Early Evolution of the Atmospheres of Terrestrial Planets, Trigo- Springer Series in Astrophysics and Space Science Proceedings, vol. 35, p. 155 (2013)
18. Balucani, N.: Elementary reactions and their role in gas-phase prebiotic chemistry. Int. J. Mol. Sci. **10**, 2304–2335 (2009)
19. Imanaka, H., Smith, M.A.: Formation of nitrogenated organic aerosols in the Titan upper atmosphere. PNAS **107**, 12423–12428 (2010)
20. Balucani, N., et al.: Dynamics of the $N(^2D)$ + $D_2$ reaction from crossed-beam and quasiclassical trajectory studies. J. Phys. Chem. A **105**, 2414–2422 (2001)
21. Balucani, N., et al.: Experimental and theoretical differential cross sections for the $N(^2D)$ + $H_2$ reaction. J. Phys. Chem. A **110**, 817–829 (2006)
22. Homayoon, Z., Bowman, J.M., Balucani, N., Casavecchia, P.: Quasiclassical trajectory calculations of the $N(^2D)$ + $H_2O$ reaction elucidating the formation mechanism of HNO and HON seen in molecular beam experiments. J. Phys. Chem. Lett. **5**, 3508–3513 (2014)
23. Balucani, N., Cartechini, L., Casavecchia, P., Homayoon, Z., Bowman, J.M.: A combined crossed molecular beam and quasiclassical trajectory study of the Titan-relevant $N(^2D)$ + $D_2O$ reaction. Mol. Phys. **113**, 2296–2301 (2015)
24. Israel, G., et al.: Complex organic matter in Titan's atmospheric aerosols from in situ pyrolysis and analysis. Nature **438**, 796 (2005)
25. Balucani, N., et al.: Combined crossed molecular beam and theoretical studies of the $N(^2D)$ + $CH_4$ reaction and implications for atmospheric models of Titan. J. Phys. Chem. A **113**, 11138–11152 (2009)
26. Balucani, N., et al.: Cyanomethylene formation from the reaction of excited nitrogen atoms with acetylene: a crossed beam and ab initio study. J. Am. Chem. Soc. **122**, 4443–4450 (2000)

27. Balucani, N., Cartechini, L., Alagia, M., Casavecchia, P., Volpi, G.G.: Observation of nitrogen-bearing organic molecules from reactions of nitrogen atoms with hydrocarbons: a crossed beam study of N($^2$D) + ethylene. J. Phys. Chem. A **104**, 5655–5659 (2000)
28. Balucani, N., et al.: Formation of nitriles and imines in the atmosphere of Titan: combined crossed-beam and theoretical studies on the reaction dynamics of excited nitrogen atoms N($^2$D) with ethane. Faraday Discuss. **147**, 189–216 (2010)
29. Balucani, N., et al.: Combined crossed beam and theoretical studies of the N($^2$D) + $C_2H_4$ reaction and implications for atmospheric models of Titan. J. Phys. Chem. A **116**, 10467–10479 (2012)
30. Vanuzzo, G., et al.: Reaction N($^2$D) + $CH_2CCH_2$ (Allene): an experimental and theoretical investigation and implications for the photochemical models of titan. ACS Earth Space Chem. **6**, 2305–2321 (2022)
31. Mancini, L., et al.: The reaction N($^2$D) + $CH_3CCH$ (methylacetylene): a combined crossed molecular beams and theoretical investigation and implications for the atmosphere of titan. J. Phys. Chem. A **125**, 8846–8859 (2021)
32. Mancini, L., de Aragao, E.V.F., Rosi, M., Skouteris, D., Balucani, N.: A theoretical investigation of the reactions of N($^2$D) with small alkynes and implications for the prebiotic chemistry of titan. In: LNCS, vol. 12251, pp. 717–729 (2020)
33. Balucani, N., Pacifici, L., Skouteris, D., Caracciolo, A., Casavecchia, P., Rosi, M.: A theoretical investigation of the reaction N($^2$D) + $C_6H_6$ and implications for the upper atmosphere of Titan. In: LNCS, vol. 10961, pp. 763–772 (2018)
34. Balucani, N., et al.: A computational study of the reaction N($^2$D) + $C_6H_6$ leading to pyridine and phenylnitrene. In: LNCS, vol. 11621, pp. 316–324 (2019)
35. Balucani, N., et al.: An experimental and theoretical investigation of the N($^2$D) + $C_6H_6$ (benzene) reaction with implications for the photochemical models of Titan. Faraday Discuss. **245**, 327351 (2023). https://doi.org/10.1039/D3FD00057E
36. Rosi M., et al.: A computational study on the attack of nitrogen and oxygen atoms to toluene. In: LNCS, vol. 12953, pp. 620–631 (2021)
37. Rosi, M., et al.: A computational study on the insertion of N($^2$D) into a C—H or C—C bond: the reactions of N($^2$D) with benzene and toluene and their implications on the chemistry of titan. In: LNCS, vol. 12251, pp. 744–755 (2020)
38. Rosi, M., et al.: A computational study of the reaction between N($^2$D) and simple aromatic hydrocarbons. In: LNCS, vol. 14105, pp. 718–734 (2023)
39. Becke, A. D.: Density functional thermochemistry. III. The role of exact exchange. J. Chem. Phys. **98**, 5648–5652 (1993)
40. Stephens, P.J., Devlin, F.J., Chablowski, C.F., Frisch, M.J.: Ab initio calculation of vibrational absorption and circular dichroism spectra using density functional force fields. J. Phys. Chem. **98**, 11623–11627 (1994)
41. Krishnan, R., Binkley, J.S., Seeger, R., Pople, J.A.: Self-consistent molecular orbital methods. XX. A basis set for correlated wave functions. J. Chem. Phys. **72**, 650–654 (1980)
42. Frisch, M.J., Pople, J.A., Binkley, J.S.: Self-consistent molecular orbital methods 25. Supplementary functions for Gaussian basis sets. J. Chem. Phys. **80**, 3265–3269 (1984)
43. Grimme, S., Ehrlich, S., Goerigk, L.: DFT-D3 - a dispersion correction for density functionals, Hartree-Fock and semi-empirical quantum chemical methods DFT-D3. J. Chem. Phys. **132**, 154104 (2010)
44. Dunning, Jr. T.H.: Gaussian basis sets for use in correlated molecular calculations. I. The atoms boron through neon and hydrogen. J. Chem. Phys. **90**, 1007–1023 (1989)
45. Gonzalez, C., Schlegel, H.B.: An improved algorithm for reaction path following. J. Chem. Phys. **90**, 2154–2161 (1989)
46. Gonzalez, C., Schlegel, H.B.: Reaction path following in mass-weighted internal coordinates. J. Phys. Chem. **94**, 5523–5527 (1990)

47. Bartlett, R.J.: Many-body perturbation theory and coupled cluster theory for electron correlation in molecules. Annu. Rev. Phys. Chem. **32**, 359–401 (1981)
48. Raghavachari, K., Trucks, G.W., Pople, J.A., Head-Gordon, M.: Quadratic configuration interaction. A general technique for determining electron correlation energies. Chem. Phys. Lett. **157**, 479–483 (1989)
49. Olsen, J., Jorgensen, P., Koch, H., Balkova, A., Bartlett, R.J.: Full configuration–interaction and state of the art correlation calculations on water in a valence double-zeta basis with polarization functions. J. Chem. Phys. **104**, 8007–8015 (1996)
50. Moore, C.E.: Atomic energy levels. Natl. Bur. Stand. (U.S.) Circ. N. 467 (U.S., GPO, Washington, DC (1949)
51. Liang, P., et al.: OH ($^2\Pi$)+ $C_2H_4$ reaction: a combined crossed molecular beam and theoretical study. J. Phys. Chem. A **127**, 4609–4623 (2023)
52. Rosi, M., et al.: Electronic structure and kinetics calculations for the $Si^+$ SH reaction, a possible route of SiS formation in star-forming regions. In: LNCS, vol. 11621, pp. 306–315 (2019)
53. Mancini, L., et al.: A computational characterization of the reaction mechanisms for the reactions N ($^2$D)+ $CH_3CN$ and $HC_3N$ and implications for the nitrogen-rich organic chemistry of Titan. Comput. Theor. Chem. **1229**, 114341 (2023)
54. Mancini, L., et al.: Destruction of interstellar methyl cyanide ($CH_3CN$) via collisions with $He^{+\cdot}$ ions. Astron. Astrophys. **691**, A83 (2024)
55. Richardson, V., et al.: Fragmentation of interstellar methanol by collisions with $He^+$: an experimental and computational study. PCCP **24**(37), 22437–22452 (2022)
56. Valença Ferreira de Aragão, E., Mancini, L., Faginas-Lago, N., Rosi, M., Skouteris, D., Pirani, F.: Semiempirical potential in kinetics calculations on the $HC_3N$+ CN reaction. Molecules **27**(7), 2297 (2022)
57. Martin, J.M.: Ab initio total atomization energies of small molecules — towards the basis set limit. Chem. Phys. Lett. **259**, 669–678 (1996)
58. Svensson, M., Humbel, S., Froese, R.D.J., Matsubara, T., Sieber, S., Morokuma, K.: ONIOM: a multilayered integrated MO + MM method for geometry optimizations and single point energy predictions. A test for Diels-Alder reactions and $Pt(P(t\text{-}Bu)_3)_2$ + $H_2$ oxidative addition. J. Phys. Chem. **100**, 19357 (1996)
59. Humbel, S., Sieber, S., Morokuma, K.: The IMOMO method: integration of different levels of molecular orbital approximations for geometry optimization of large systems: test for n-butane conformation and SN2 reaction: RCl+$Cl^-$. J. Chem. Phys. **105**, 1959 (1996)
60. Maseras, F., Morokuma, K.: IMOMM: a new integrated ab initio + molecular mechanics geometry optimization scheme of equilibrium structures and transition states. J. Comp. Chem. **16**, 1170 (1995)
61. Frisch, M. J., et al.: Gaussian 09, Revision A.02. Gaussian, Inc., Wallingford CT (2009)
62. Werner, H.-J., Knowles, P.J., Knizia, G., Manby, F.R., Schütz, M.: Molpro: a general-purpose quantum chemistry program package. WIREs Comput. Mol. Sci. **2**, 242–253 (2012)
63. Werner, H.-J., et al.: The Molpro quantum chemistry package. J. Chem. Phys. **152**, 144107 (2020)
64. Flükiger, P., Lüthi, H.P., Portmann, S., Weber, J., MOLEKEL 4.3, Swiss Center for Sci-entific Computing, Manno (Switzerland), 2000–2002
65. Portmann, S., Lüthi, H. P., MOLEKEL: an interactive molecular graphics tool Chimia **54**, 766–769 (2000)
66. Mancini, L., Balucani, N., Rosi, M.: The reaction of N($^2$D) with monocyclic and polycyclic aromatic hydrocarbons and their role in the atmospheric chemistry of Titan. Icarus, **457**, 117152 (2026)